

Full Paper

Visualization and characterization of spore morphogenesis in *Paenibacillus polymyxa* ATCC39564

(Received July 29, 2021; Accepted October 25, 2021; J-STAGE Advance publication date: April 13, 2022)

Kimihiko Abe,¹ Hiroko Kato,² Yuta Hasegawa,² Tatsuya Yamamoto,¹
Nobuhiko Nomura,^{1,3,*} and Nozomu Obana^{3,4,*}

¹ Faculty of Life and Environmental Sciences, University of Tsukuba, 1-1-1 Ten-nodai, Tsukuba, Ibaraki, Japan

² Graduate School of Life and Environmental Sciences, University of Tsukuba, 1-1-1 Ten-nodai, Tsukuba, Ibaraki, Japan

³ Microbiology Research Center for Sustainability, University of Tsukuba, 1-1-1 Ten-nodai, Tsukuba, Ibaraki, Japan

⁴ Transborder Medical Research Center, Faculty of Medicine, University of Tsukuba, 1-1-1 Ten-nodai, Tsukuba, Ibaraki, Japan

Paenibacillus polymyxa is a spore-forming Gram-positive bacterial species. Both its sporulation process and the spore properties are poorly understood. Here, we investigated sporulation in *P. polymyxa* ATCC39564. When cultured at 37°C for 24 h in sporulation medium, more than 80% of the total cells in the culture were spores. Time-lapse imaging revealed that cellular morphological changes during sporulation of *P. polymyxa* were highly similar to those of *B. subtilis*. We demonstrated that genetic deletion of *spo0A*, *sigE*, *sigF*, *sigG*, or *sigK*, which are highly conserved transcriptional regulators in spore-forming bacteria, abolished spore formation. In *P. polymyxa*, *spo0A* was required for cell growth in sporulation medium, as well as for the initiation of sporulation. The *sigE* and *sigF* mutants formed abnormal multiple asymmetric septa during the early stage of sporulation. The *sigG* and *sigK* mutants formed forespores in the sporangium, but they did not become mature. Moreover, fluorescence reporter analysis confirmed compartment-specific gene expression of *spoIID* and *spoVFA* in the mother cell and *spoIIQ* and *sspF* in the forespore. Transmission electron microscopy imaging revealed that *P. polymyxa* produces multi-layered endospores but lacking a balloon-shaped exosporium. Our results indicate that spore morphogenesis is conserved between *P. polymyxa* and *B. subtilis*. However, *P. polymyxa* genomes lack many

homologues encoding spore-coat proteins that are found in *B. subtilis*, suggesting that there are differences in the spore coat composition and surface structure between *P. polymyxa* and *B. subtilis*.

Key Words: *Paenibacillus polymyxa*; cellular differentiation; sporulation; endospore; sporulation-specific sigma factors

Introduction

Sporulation is an adaptation strategy in bacteria to survive harsh environmental conditions by transforming into endospores, which are metabolically dormant and highly resistant to various stresses (Beskrovnaya *et al.*, 2021). Bacterial sporulation has been intensely studied in *Bacillus subtilis*, which has a simple process of cellular differentiation (Errington, 2003; Higgins and Dworkin, 2012). Sporulation is initiated with an asymmetric cell division when the environment becomes adverse, such as when nutrients are exhausted. Consequently, two types of cell compartments that differ in size are generated; the smaller compartment is a forespore that develops into the endospore, while the larger cell is called the mother cell and supports spore development. After the formation of the asymmetric septum, engulfment of the forespore into the mother cell cytosol takes place, assisted by a peptidoglycan remodeling enzyme complex, SpoIIM-SpoIID-SpoIIP (Khanna *et al.*, 2019). Substrates necessary for the subsequent stage

*Corresponding authors: Nobuhiko Nomura, Microbiology Research Center for Sustainability, University of Tsukuba, 1-1-1 Ten-nodai, Tsukuba, Ibaraki 305-8577, Japan; and Nozomu Obana, Microbiology Research Center for Sustainability, University of Tsukuba, 1-1-1 Ten-nodai, Tsukuba, Ibaraki 305-8577, Japan.

Tel: +81-29-853-6627 E-mail: nomura.nobuhiko.ge@u.tsukuba.ac.jp

Tel: +81-29-853-3213 E-mail: obana.nozomu.gb@u.tsukuba.ac.jp

None of the authors of this manuscript has any financial or personal relationship with other people or organizations that could inappropriately influence their work.

can be trafficked between the mother cell and the forespore through a SpoIIAH-SpoIIQ channel (Levdikov *et al.*, 2012; Meisner *et al.*, 2012). During spore development, dipicolinic acid (DPA) and small acid-soluble proteins (SASPs) accumulate in the forespore and provide the spore with resistance against heat and UV irradiation (Setlow *et al.*, 2006; Beskrovnaya *et al.*, 2021). DPA is synthesized by the SpoVFA-SpoVFB complex in the mother cell and is then transported into the spore compartment through DPA transporters, SpoVA (Tovar-Rojo *et al.*, 2002) and SpoVV (Ramírez-Guadiana *et al.*, 2017). DPA accumulation leads to the dehydration of the inside of the spore, providing heat resistance (Balassa *et al.*, 1979). SASPs are expressed from multiple *ssp* genes in the forespore, which are DNA-binding proteins that protect spore DNA from UV damage. In the mother cell compartment, peptidoglycan synthesis is activated to form the cortex layer, and then a number of spore-coat proteins, more than 70 in *B. subtilis*, are synthesized and attached to the spore surface, forming multiple spore-coat layers (McKenney *et al.*, 2013; Driks and Eichenberger, 2016). At the final stage, the mother cell lyses to release the mature spore.

Expression of sporulation-related genes is governed by sporulation-specific transcriptional regulators that are conserved among spore-forming bacteria. In the transition from vegetative to sporulating cells, Spo0A acts as the master transcriptional factor for entry into sporulation. When the environment becomes adverse, Spo0A is activated through phosphorylation. Phosphorylated Spo0A upregulates early sporulation genes such as *sigH*, *sigE*, and *sigF*. After the asymmetric cell division, gene expression is governed by four temporal sporulation- and compartment-specific sigma factors: SigE in the early phase of the mother cell, SigK in the late phase of the mother cell, SigF in the early phase of the forespore, and SigG in the late phase of the forespore. The genetic program of sporulation proceeds via communication between the forespore and the mother cell (Losick and Stragier, 1992; Rudner and Losick, 2001), in which the sigma factors are activated in the order SigF, SigE, SigG, and SigK. This cascade of sigma factors enables a successful progression of the genetic program to generate an endospore, which is highly conserved across the spore-forming Firmicutes including *Bacillus* spp and *Clostridium* spp (Fimlaid and Shen, 2015).

Paenibacillus polymyxa (formerly *Bacillus polymyxa*) is a Gram-positive bacterial species (Ash *et al.*, 1993) known to colonize plant roots and promote the growth of plants (Lal and Tabacchioni, 2009). *P. polymyxa* is often isolated from raw milk and dairy foods and can cause food spoilage and poisoning (Gopal *et al.*, 2015). Contamination with this bacterium is a significant issue in the food industry. *P. polymyxa* cells can also form endospores that show extremely high resistance to various stresses, and this property allows them to survive disinfection in food processing (Huo *et al.*, 2012). Therefore, a deeper understanding of the sporulation of this bacterial species is essential for their biocontrol. However, the fundamentals of sporulation in *P. polymyxa* remain poorly understood. In this study, we investigated the sporulation process of the *P. polymyxa* strain ATCC39564, focusing on imaging of

the cell morphology and validation of the function of sporulation regulators.

Materials and Methods

Bacterial strains and culture conditions. The bacterial strains and plasmids used are listed in Table S1. The oligonucleotides used in this study are shown in Table S2. Details of *P. polymyxa* strain construction are provided in the Supplementary Materials. *P. polymyxa* strains were cultured at 37°C under routine shaking in Tryptone-Soy Broth (TSB; Difco).

Sporulation. An aliquot of TSB-overnight subculture of *P. polymyxa* (100 μ l) was inoculated into fresh 4-ml Difco sporulation medium (DSM; 8 g/l Difco nutrient broth, 0.49 mM MgCl₂, 13.4 mM KCl, 1 mM Ca(NO₃)₂, 10 μ M MnCl₂, and 1 μ M FeSO₄) and was then cultured at 37°C to induce sporulation. Cell growth of both the wild-type (WT) and mutants was measured using a multimode microplate reader (Cytation 5, BioTek). The sporulation efficiency was determined as described previously (Abe *et al.*, 2013), with the following modifications: heat treatment at 70°C for 30 min and use of TSB-agar plates.

Time-lapse imaging. Overnight subcultures of *P. polymyxa* strains were inoculated in 4 ml of liquid DSM and grown at 37°C for 4 h. Subsequently, 1 ml of the culture was centrifuged at 20,400 \times g for 1 min. The culture supernatant was filtered through a 0.22- μ m PVDF membrane (Millipore). The filtered supernatant (75 μ l) was mixed with 1 μ l of 1 mg/ml FM1-43 (Thermo Fisher Scientific) and 25 μ l of melted 4% agarose solution (Agarose H, Nippon Gene). After the agar pad solidified on a slide glass, sporulating cells were mounted on the pad and observed with a Zeiss LSM780 confocal laser microscope equipped with an EC Plan-Neofluar 100 \times /1.3 Oil Ph3 M27 objective lens (Zeiss), a T-PMT detector for phase-contrast images, a 488-nm laser generator, and an AiryScan detector (BP495–550 + LP570 emission filter) to obtain confocal fluorescence images. The agar pad was incubated at 37°C during observation. Images were processed using Zen Blue edition v. 2.3 (Zeiss) and Image J Fiji v. 1.53c (Schindelin *et al.*, 2012).

Transmission electron microscopy. Sporulating cells and purified spores were fixed with 2.5% glyceraldehyde overnight at 4°C. Ethanol dehydration was performed by increasing the ethanol concentration stepwise as follows: 50%, 70%, 90%, and 100%. Fixed and dehydrated samples were embedded in epoxy resin using an Oken Epok 812 set (Oken). Ultra-thin sections were prepared using a Leica EM UC7 microtome with an ultra 45° diamond knife (DiATOME Ltd.). Ultra-thin sections were mounted onto carbon-coated grids (Catalogue No. 649, Nisshin EM) and were stained with EM stain (Nisshin EM) and Reynolds' stain (Reynolds, 1963). Imaging was performed with the transmission electron microscope H7650 (Hitachi High-Technologies Corporation).

Fluorescence microscopy. The construction of green fluorescence reporter plasmids is described in the Supplementary Methods. Overnight subcultures of *P. polymyxa*

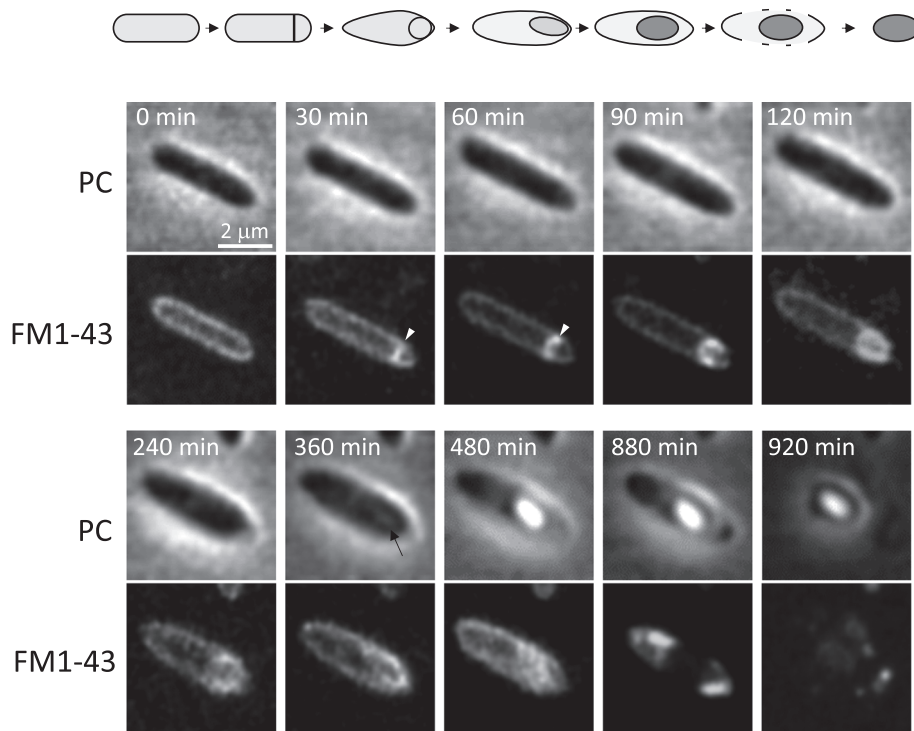


Fig. 1. Morphological changes during sporulation in *P. polymyxa* ATCC39564.

The schematic shows typical morphological changes during sporulation in *P. polymyxa*. A sporulating WT cell on a DSM-agar pad was observed with phase-contrast and confocal laser microscopy. Representative images from two independent experiments are shown. Images were taken at the indicated time points on the panel. The white arrowhead and black arrow indicate the asymmetric septum and phase-dark forespore, respectively. PC, phase contrast; FM1-43 (emission/excitation wavelengths = 488/580 nm), membrane staining. Scale bar, 2 μm .

strains carrying these plasmids were spotted onto DSM-agar plates containing 1 $\mu\text{g/ml}$ erythromycin and were then cultured at 37°C for 16 h. Sporulating cells were scrapped from the agar plates and resuspended with PBS containing 5 $\mu\text{g/ml}$ FM4-64 (Thermo Fisher Scientific). The sporulating cells were observed with phase-contrast microscopy and fluorescence microscopy (Zeiss Axio observer equipped with an EC Plan-Neofluar 100 \times /1.3 Oil Ph3 M27 objective lens (Zeiss) and dichroic filters for green (excitation/ emission wavelengths, 450–490/500–550 nm) and red (538–562/570–640 nm) fluorescent proteins).

Purification of spores. Overnight TSB-subculture of WT *P. polymyxa* (200 μl) was spread on a DSM-agar plate and was then incubated at 37°C for 5 d to allow sporulation and lysis of non-sporulating cells. The spores were purified as described previously (Abe *et al.*, 2014) with centrifugation at 500 $\times g$ for 5 min as a modification. The purified spores were suspended in DDW.

Results and Discussion

Sporulation of *P. polymyxa*

At the beginning of this study, we examined three media for induction of a *P. polymyxa* strain, ATCC39564 (hereafter referred to as the WT). The WT strain was cultured at 37°C for 24 h under aerobic conditions in 4 ml of either DSM, 2 \times SG (Leighton and Doi, 1971), or TSB supplemented with minerals [0.49 mM MgCl_2 , 13.4 mM KCl, 1 mM $\text{Ca}(\text{NO}_3)_2$, 10 μM MnCl_2 , and 1 μM FeSO_4]. *P. polymyxa*

cells formed mature spores only in DSM under our conditions (Fig. S1). Therefore, we used DSM in this study, although the cell growth of *P. polymyxa* in this medium was much poorer than that of *B. subtilis*. To visualize the morphological changes that occurred during sporulation, we performed time-lapse imaging of WT *P. polymyxa*. Figure 1 shows the morphological change of a typical cell in the population. An asymmetric septum appeared 30 min after the start of observation. Engulfment of the forespore into the mother cell completed within the next 90 min (30–120 min). As the spherical forespore shaped into an ellipse, it was detectable as a phase-dark forespore by phase-contrast microscopy (at 360 min). Subsequently, the forespore became phase bright and moved toward the center of the mother cell (by 480 min). There were no apparent morphological changes from this state until the release of the mature spore. Finally, the mother cell lysed to release the mature spore (880–920 min). As we demonstrated, the spore formation of *P. polymyxa* progressed in a similar manner to that of *B. subtilis* (Errington, 1993). However, unlike *B. subtilis*, we observed that the sporulating cell enlarged, forming the spindle-shaped sporangium. Typically, the region of the mother cell near the forespore expands after engulfment has completed, as shown in Figure 1. However, in some populations, this enlargement occurred at the initiation of sporulation or in the center of the mother cell (data not shown). Additionally, *P. polymyxa* showed heterogeneity in the length of the sporangia (Fig. S2), ranging from approximately 3.5 to 7.5 μm (typically,

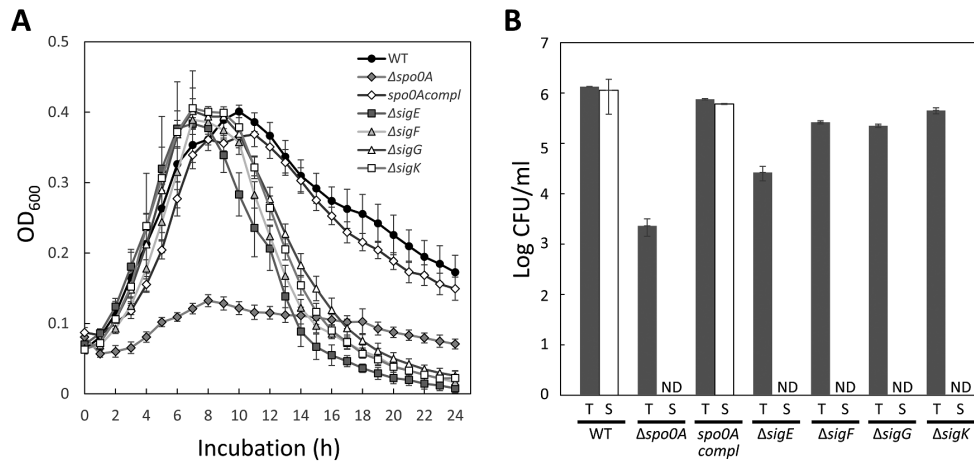


Fig. 2. Sporulation deficiencies in the $\Delta spo0A$, $\Delta sigE$, $\Delta sigF$, $\Delta sigG$, and $\Delta sigK$ mutants.

A. Cell growth. *P. polymyxa* WT (filled circle), $\Delta spo0A$ (open diamond), $\Delta spo0A$ complemented with pAMYE-*spo0A* (*spo0A_{compl}*; filled diamond), $\Delta sigE$ (filled square), $\Delta sigF$ (filled triangle), $\Delta sigG$ (open triangle), and $\Delta sigK$ (open square) strains were cultured at 37°C in 100 μ l DSM in a 96-well plate with shaking. The OD₆₀₀ value was monitored hourly using a multimode plate reader. Means were plotted with standard deviations ($n = 6$). **B.** Colony formation units (CFUs). The *P. polymyxa* strains were cultured at 37°C for 24 h in 4 ml DSM. Numbers of total cells (T; grey bar) and heat-resistant spores (S; white bar) in the cultures were determined by counting the colonies on TSB-agar plates. Means of the CFUs were plotted with standard deviations, based on three independent experiments. ND, not detected.

4.5–5.0 μ m, $n = 78$), although the underlying cause of these morphological differences remains to be determined. Additionally, it is unknown whether these morphological differences between sporangia exert an influence on the properties of the spore.

Impact of knockout of *spo0A*, *sigE*, *sigF*, *sigG*, and *sigK* on sporulation

In *B. subtilis*, the initiation and progression of sporulation are controlled by Spo0A and four sporulation-specific sigma factors (Errington, 2003; Higgins and Dworkin, 2012). These key sporulation regulators are also conserved in *P. polymyxa*. *P. polymyxa* ATCC39564 Spo0A, SigE, SigF, SigG, and SigK have 68.8%, 77.6%, 73.4%, 79.5%, and 71.2% identity to those from *B. subtilis*, respectively. Unlike *B. subtilis* 168 and *Clostridioides difficile* 630, *P. polymyxa sigK* has no gene-intervening element (called *skin*), which is excluded from the mother cell genome during sporulation (Stragier *et al.*, 1989; Sato *et al.*, 1990; Serrano *et al.*, 2016). We constructed deletion mutants of each of these regulator genes to validate their roles in sporulation. When cultured in DSM, the cell growth of WT peaked at 10 h after the inoculation and gradually decreased at later time points (Fig. 2A). None of the deletion mutants, except for the deletion mutant of *spo0A* ($\Delta spo0A$), caused severe defects in cell proliferation. To confirm the unexpected growth-deficient phenotype of $\Delta spo0A$, we constructed a *spo0A*-complemented strain, in which *spo0A* and kanamycin resistance genes were inserted into the *amyE* locus through a double crossing over event (as described in Supplementary Methods). The growth defects in $\Delta spo0A$ was recovered by the genetic complementation of *spo0A* (Fig. 2A, *spo0A_{compl}*), indicating that Spo0A is necessary for the cell growth in DSM. In *P. polymyxa* ATCC39564, Spo0A regulatory network may therefore involve genes for cell proliferation as well as sporula-

tion-related genes. The WT showed a higher OD value at 24 h than the mutants due to the presence of spores after the mother cell lysed. The WT 24-h culture exhibited 1.1×10^6 CFU/ml of heat resistance spores, which was 84.3% of the total viable cells (Fig. 2B). In contrast to the WT, the mutants showed much lower total CFUs (2.3×10^3 – 4.5×10^5 /ml) and produced no heat-resistant spores under our culture conditions. These results indicate that SigE, SigF, SigG, and SigK are essential for sporulation in *P. polymyxa*. As shown in Figure 2B, the *spo0A_{compl}* cells sporulated (0.61×10^6 CFU/ml of heat resistance spores), while the $\Delta spo0A$ cells did not, suggesting that Spo0A is required for the initiation of sporulation. However, we could not rule out the possibility that the $\Delta spo0A$ cells could not enter sporulation because nutrient exhaustion did not occur since there was a low cell density. Recently, Hou *et al.* reported that an amino acid mutation at arginine residue 211 of *P. polymyxa* Spo0A led to defects in the transcription of sporulation-related genes and in spore formation without severe growth defects (Hou *et al.*, 2016). This supports the notion that *P. polymyxa* Spo0A regulates sporulation.

Cell morphology of sporulation-deficient mutants during sporulation

We performed time-lapse imaging of sporulation-deficient mutants to examine which sporulation processes were blocked in each mutant. First, the *spo0A* mutant did not enter the sporulation process or proliferate (Fig. 3). Progression of sporulation in the $\Delta sigE$ and $\Delta sigF$ mutants was arrested at the early stage of sporulation. These mutants retained the ability to form the asymmetric septum. However, the septum was formed at both cell poles (Fig. 3) and, subsequently, the cells lysed. Engulfment took place in the $\Delta sigG$ and $\Delta sigK$ mutants (Fig. 3, 120 min), but their forespores were undetectable or phase-dark under

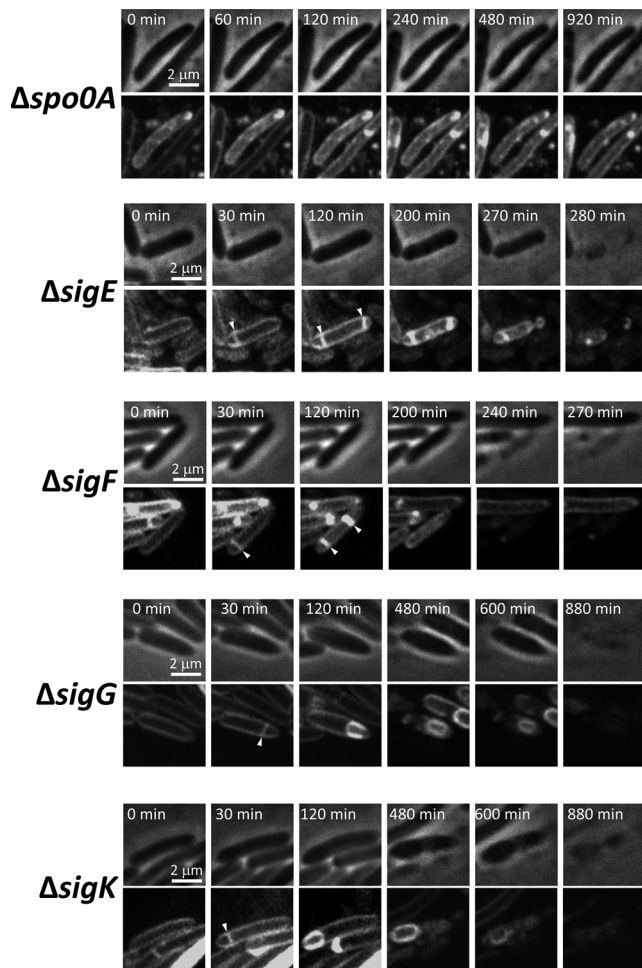


Fig. 3. Time-lapse imaging of sporulation-deficient mutants.

The $\Delta spo0A$, $\Delta sigE$, $\Delta sigF$, $\Delta sigG$, and $\Delta sigK$ mutant cells on DSM-agar pads were observed with phase contrast and confocal laser microscopy. Pictures were taken at the indicated time points on the panel. Representative images from two independent experiments are shown. Arrow heads point to the septa. Upper panels, phase-contrast images; bottom panels, FM1-43, fluorescence images (emission/excitation wavelengths = 488/580 nm). Scale bar, 2 μ m.

phase-contrast microscopy (480 min). The mutant sporangia eventually lysed without producing mature spores.

Transmission electron microscopy (TEM) imaging of ultra-thin sections of the sporulating cells clarified the morphological differences between the WT and mutants in more detail. The upper panels of Figure 4 show a WT cell at the early stage that completed the asymmetric septum formation and the $\Delta sigE$ and $\Delta sigF$ mutants, which generated the septum at both cell poles. Multiple abnormal septa were formed at a single cell pole in the $\Delta sigE$ and $\Delta sigF$ mutants (Fig. S3). The $\Delta spo0A$ mutant did not form an asymmetric septum (Fig. S4). At the middle stage of sporulation, the WT sporangium created a forespore that formed the spore core, cortex, and spore-coat layers (Fig. 4). Both the $\Delta sigG$ and $\Delta sigK$ mutant sporangia formed a forespore without the cortex or spore-coat layers. Meanwhile, the forespore produced in the $\Delta sigK$ sporangium was more electron-dense than that of the $\Delta sigG$ mutant, probably due to the expression of SigG-controlled genes in the $\Delta sigK$ forespore. Taken together, these results provide evidence that SigE and SigF govern the progression of

sporulation at the early stage while SigG and SigK govern sporulation at the later stages.

Compartment-specific gene expression during sporulation

An important feature in the bacterial sporulation process is compartment-specific gene expression. To examine this, we constructed reporter plasmids in which a green fluorescent protein gene *ZsGreen* is under the control of sporulation-gene-specific promoters: the P_{spoIID} promoter (P_{spoIID}) for SigE, P_{spoIIQ} for SigF, P_{sspF} for SigG, and P_{spoVFA} for SigK. The predicted promoter sequences are shown in Table S3. The reporter plasmids were introduced into WT *P. polymyxa* cells. Since the plasmid-carrying cells did not sporulate in liquid DSM containing erythromycin for unknown reasons, they were cultured on DSM-agar plates containing antibiotics. We observed that the P_{spoIID} and P_{spoVFA} promoters were activated in the mother cell compartment, while the P_{spoIIQ} and P_{sspF} promoters were activated in the forespore compartment (Fig. 5). This data suggests that SigE and SigK exert gene regulatory functions in the mother cell compartment, while SigF and SigG act in the forespore. The dependence of the promoters on sporulation-specific sigma factors was confirmed using the mutants carrying these plasmids (Fig. S5). Taken together with our results from the morphological analysis, we conclude that *P. polymyxa* sporulation-specific sigma factors are structurally and functionally homologous to those of *Bacillus* (e.g. *B. subtilis*, *B. anthracis*, and *B. cereus*) and *Clostridium* and the closely-related species (e.g. *C. acetobutylicum*, *C. botulinum*, and *C. difficile*) (Fimlaid and Shen, 2015), although the details of the mechanisms of sigma factor activation and their regulons remain to be elucidated.

Spore morphology

To directly observe *P. polymyxa* mature spores, we performed TEM imaging on ultra-thin sections of the spores. The TEM images revealed that *P. polymyxa* WT spores have a multilayered structure consisting of the spore core (CO), cortex (CR), lamella-like inner spore-coat (IC), and outer spore-coat (OC) layers (Fig. 6). Like *B. subtilis* spores, *P. polymyxa* spores have no appendage such as Ena that is found in *B. cereus sensu lato* (Pradhan *et al.*, 2021) and no exosporium separated from the spore coats by an interspace which is a balloon-like structure observed in some *Bacillus* species including *B. anthracis* and *B. cereus* (Stewart, 2015). Thus, the *P. polymyxa* spores resemble those from *B. subtilis* (McKenney *et al.*, 2013; Driks and Eichenberger, 2016). Despite this structural similarity, many of the spore-coat proteins in *B. subtilis* are not shared with *P. polymyxa*, while the spore morphogenic proteins, SpoIVA, SpoVM, SpoVID, SafA, and CotE, are highly conserved. Out of 84 *B. subtilis* spore proteins analyzed here, only 32–36 were conserved in three *P. polymyxa* strains (Table S4). Given that the spore-coat proteins play the important roles in spore protection and germination, the *P. polymyxa* spores could have different characteristics from *B. subtilis* spores.

As shown in Figure 6, the *P. polymyxa* outer spore-coat layer could be further subdivided into two: an inside layer

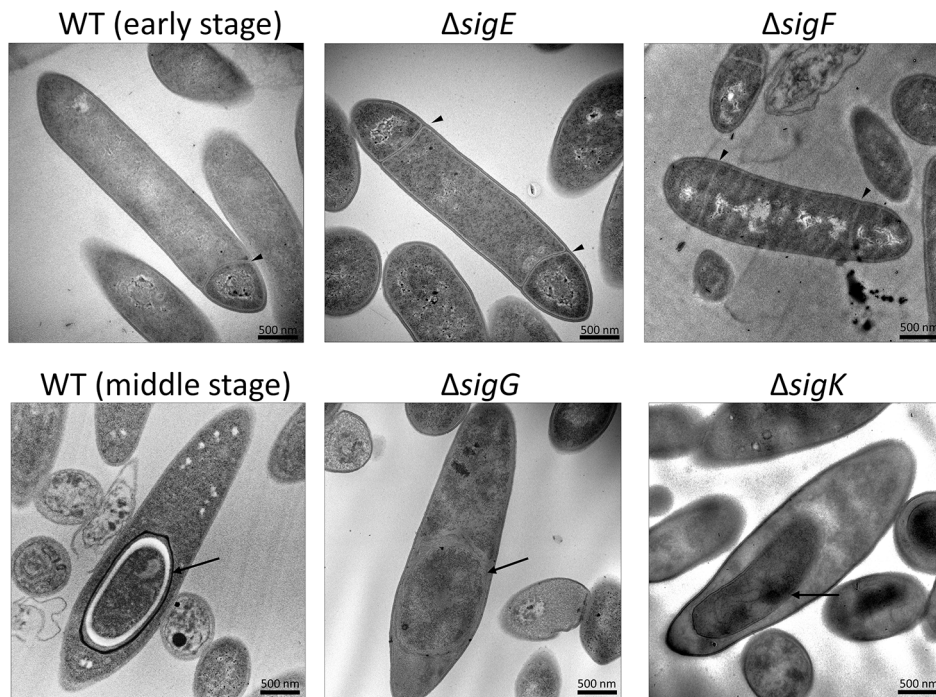


Fig. 4. Morphological observation of *P. polymyxa* spores by TEM.

P. polymyxa WT, $\Delta sigE$, $\Delta sigF$, $\Delta sigG$, and $\Delta sigK$ were cultured at 37°C for 7.5 h (early stage) and 14 h (middle stage) in DSM, and then they were fixed and embedded in epoxy resin. Ultra-thin sections of the sporulating cells were observed with TEM. Arrow heads (early phase) and arrows (middle stage) indicate the asymmetric septa and forespores, respectively. Scale bar, 500 nm.

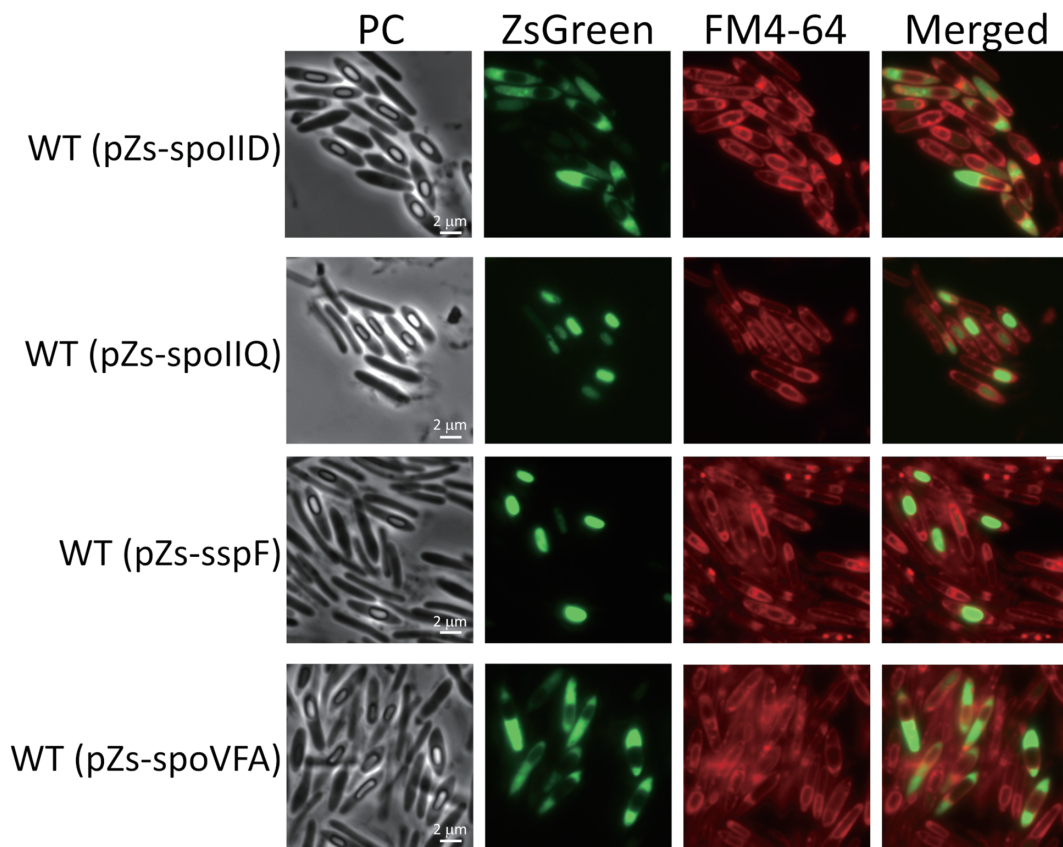


Fig. 5. Compartment-specific gene expression during sporulation.

Green fluorescence reporter plasmids carrying *ZsGreen* under promoters controlled by SigE (pZs-spoIID), SigF (pZs-spoIIQ), SigG (pZs-sspF), and SigK (pZs-spoVFA) were introduced into *P. polymyxa* WT. The *P. polymyxa* cells harboring these plasmids were cultured at 37°C for 16 h on DSM-agar plates. The cells were stained with FM4-64 and subjected to observation with phase-contrast and fluorescence microscopy. PC, phase contrast; ZsGreen, green fluorescent reporter protein (emission/excitation wavelengths = 493/505 nm); FM4-64, membrane staining (emission/excitation wavelengths = 515/640 nm); Merged, merged images of ZsGreen and FM4-64. Scale bar, 2 μ m.

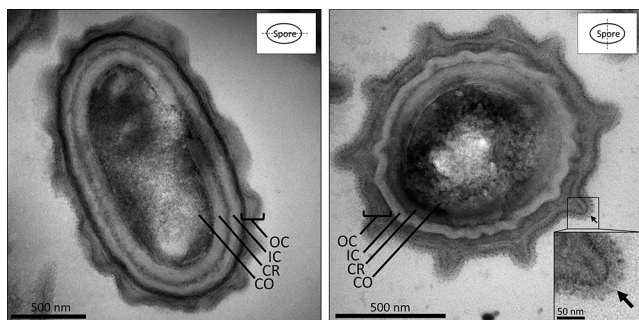


Fig. 6. Spore morphology.

Ultra-thin sections of the purified *P. polymyxa* WT spores were observed with TEM. Cutting lines in the schematic indicate the direction of the section. The arrow indicates the spore surface materials. CO, spore core; CR, cortex; IC, inner spore-coat layer; OC, outer spore-coat layer. Scale bars are indicated on each panel.

attached on the inner spore coat and a spore-surface wavy layer. Zhang and colleagues, who have reported the ultra-structure of *P. polymyxa* ShX301 sporangia, have referred to these layers as the middle and outer spore coats, respectively (Zhang *et al.*, 2018). In *B. subtilis*, the spore outer coat layer is surrounded by the spore crust, which is the outermost proteinous layer attached with polysaccharides (McKenney *et al.*, 2010; Abe *et al.*, 2014; Shuster *et al.*, 2019a; Shuster *et al.*, 2019b). Since *P. polymyxa* has no homologues to the crust layer proteins CotX, CotY, and CotZ, it is unclear whether the spore surface layer of *P. polymyxa* corresponds to the *B. subtilis* crust. Notably, the *P. polymyxa* spore surface layer is covered with uncharacterized components (Fig. 6, arrow on right panel). In *B. anthracis*, the surface of the exosporium is covered with glycosylated BclA protein, which is a collagen-like protein containing many G-X-X (mainly G-P-T) amino acid residue repeats (Stewart, 2015). We found that *P. polymyxa* (strains ATCC39564 and M1) also possesses a gene encoding a collagen-like protein (PclA, *P. polymyxa* collagen-like protein A) containing G-X-Q (GPQ, GAQ, GVQ, or GDQ) repeats (Fig. S6A), although PclA showed no significant homology with BclA. Because a putative SigK-controlled promoter was found upstream of the *pclA*-coding region (Fig. S6B), there could be the possibility that PclA is a spore-coat protein. To address the possibility, we constructed a *P. polymyxa* strain expressing a PclA-mScarlet-I fusion protein under the putative SigK-controlled promoter, in which the N-terminal region of PclA (positions 1–121) was fused with mScarlet-I, since we could not clone the entire *pclA* gene probably due to the 3' repeated sequences (encoding G-X-P repeats). When this strain was induced to sporulate on a DSM-agar plate, red fluorescence was detected around the spores (Fig. S6C). This result suggests that PclA is a novel spore-coat protein of *P. polymyxa* ATCC39564, which does not exist in *B. subtilis* 168. However, it remains unclear whether PclA is localized on the spore surface. Further investigation of the *P. polymyxa* spore surface will be required.

Conclusions

In this study, we characterized sporulation of *P. polymyxa* ATCC39564 and demonstrated the morphological changes

during sporulation. Our findings are as follows: 1) *P. polymyxa* exhibited the poor growth in DSM. 2) *P. polymyxa* Spo0A is necessary for cell growth, as well as for sporulation in DSM. 3) the cascade of four sporulation-specific sigma factors is conserved in *P. polymyxa*. 4) the spore structure resembles to those of *B. subtilis* in terms of the multilayered spore coats and the absence of balloon-shaped exosporium and spore appendages. 5) many of *B. subtilis* spore-coat proteins are missing in *P. polymyxa*. 6) PclA was identified as a novel spore coat protein in *P. polymyxa* ATCC39564.

The poor growth in DSM and the Spo0A requirement for proliferation may represent the unique nutritional utilization of *P. polymyxa*. A knowledge of the optimal and adverse growth conditions for *P. polymyxa* will be valuable for biocontrol of their propagation. Our genomic analysis implies that the spore coat of the *P. polymyxa* spore is largely composed of uncharacterized proteins, including PclA. Those unknown spore-coat components probably characterize spore properties such as resistance and interaction with the environments. Investigation of the spore-coat proteins and their roles in spore protection is essential to develop effective disinfection methods for *Paenibacillus* species. Further structural and functional analyses on *P. polymyxa* spore proteins will be needed for a better understanding of the ecology of *P. polymyxa* and for biocontrol against this bacterial species in the food industry.

Acknowledgments

This work was supported by the Japan Science and Technology Agency [ERATO JPMJER1502 to NN] and by Japan Society for the Promotion of Science (KAKEN-HI, grant number 19K05762 and 21K07018 to NO). We thank Yuko Nakayama for technical assistance. We thank Kazuya Morikawa for the gift of the pMAD plasmid.

Statement

The authors declare no conflict of interest.

Supplementary Materials

Supplementary materials are available online (<http://www.jstage.jst.go.jp/browse/jgam>)

References

- Abe, K., Kawano, Y., Iwamoto, K., Arai, K., Maruyama, Y., Eichenberger, P., and Sato, T. (2014) Developmentally-regulated excision of the SPB prophage reconstitutes a gene required for spore envelope maturation in *Bacillus subtilis*. *PLoS Genet.*, **10**, e1004636.
- Abe, K., Yoshinari, A., Aoyagi, T., Hirota, Y., Iwamoto, K., and Sato, T. (2013) Regulated DNA rearrangement during sporulation in *Bacillus weihenstephanensis* KBAB4. *Mol. Microbiol.*, **90**, 415–427.
- Ash, C., Priest, F.G., and Collins, M.D. (1993) Molecular identification of rRNA group 3 bacilli (Ash, Farrow, Wallbanks and Collins) using a PCR probe test. Proposal for the creation of a new genus *Paenibacillus*. *Antonie Van Leeuwenhoek*, **64**, 253–260.
- Balassa, G., Milhaud, P., Raulet, E., Silva, M.T., and Sousa, J.C. (1979) A *Bacillus subtilis* mutant requiring dipicolinic acid for the development of heat-resistant spores. *J. Gen. Microbiol.*, **110**, 365–379.
- Beskrovnaya, P., Sexton, D.L., Golmohammadzadeh, M., Hashimi, A., and Tocheva, E.I. (2021) Structural, metabolic and evolutionary comparison of bacterial endospore and exospore formation. *Front. Microbiol.*, **12**, 630573.
- Driks, A. and Eichenberger, P. (2016) The spore coat. *Microbiol. Spectr.*, **4**.

- Errington, J. (1993) *Bacillus subtilis* sporulation: regulation of gene expression and control of morphogenesis. *Microbiol. Rev.*, **57**, 1–33.
- Errington, J. (2003) Regulation of endospore formation in *Bacillus subtilis*. *Nat. Rev. Microbiol.*, **1**, 117–126.
- Fimlaid, K.A. and Shen, A. (2015) Diverse mechanisms regulate sporulation sigma factor activity in the Firmicutes. *Curr. Opin. Microbiol.*, **24**, 88–95.
- Gopal, N., Hill, C., Ross, P.R., Beresford, T.P., Fenelon, M.A., and Cotter, P.D. (2015) The prevalence and control of *Bacillus* and related spore-forming bacteria in the dairy industry. *Front. Microbiol.*, **6**, 1418.
- Higgins, D. and Dworkin, J. (2012) Recent progress in *Bacillus subtilis* sporulation. *FEMS Microbiol. Rev.*, **36**, 131–148.
- Hou, X., Yu, X., Du, B., Liu, K., Yao, L., Zhang, S., Selin, C., Fernando, W.G., Wang, C., and Ding, Y. (2016) A single amino acid mutation in Spo0A results in sporulation deficiency of *Paenibacillus polymyxa* SC2. *Res. Microbiol.*, **167**, 472–479.
- Huo, Z., Zhang, N., Raza, W., Huang, X., Yong, X., Liu, Y., Wang, D., Li, S., Shen, Q., and Zhang, R. (2012) Comparison of the spores of *Paenibacillus polymyxa* prepared at different temperatures. *Biotechnol. Lett.*, **34**, 925–933.
- Khanna, K., Lopez-Garrido, J., Zhao, Z., Watanabe, R., Yuan, Y., Sugie, J., Pogliano, K., and Villa, E. (2019) The molecular architecture of engulfment during *Bacillus subtilis* sporulation. *eLife*, **8**, e45257.
- Lal, S. and Tabacchioni, S. (2009) Ecology and biotechnological potential of *Paenibacillus polymyxa*: a minireview. *Indian J. Microbiol.*, **49**, 2–10.
- Leighton, T.J. and Doi, R.H. (1971) The stability of messenger ribonucleic acid during sporulation in *Bacillus subtilis*. *J. Biol. Chem.*, **246**, 3189–3195.
- Levdikov, V.M., Blagova, E.V., McFeat, A., Fogg, M.J., Wilson, K.S., and Wilkinson, A.J. (2012) Structure of components of an intercellular channel complex in sporulating *Bacillus subtilis*. *Proc. Nat. Acad. Sci. U. S. A.*, **109**, 5441–5445.
- Losick, R. and Stragier, P. (1992) Crisscross regulation of cell-type-specific gene expression during development in *B. subtilis*. *Nature* **355**, 601–604.
- McKenney, P.T., Driks, A., and Eichenberger, P. (2013) The *Bacillus subtilis* endospore: assembly and functions of the multilayered coat. *Nat. Rev. Microbiol.*, **11**, 33–44.
- McKenney, P.T., Driks, A., Eskandarian, H.A., Grabowski, P., Guberman, J., Wang, K.H., Gitai, Z., and Eichenberger, P. (2010) A distance-weighted interaction map reveals a previously uncharacterized layer of the *Bacillus subtilis* spore coat. *Curr. Biol.*, **20**, 934–938.
- Meisner, J., Maehigashi, T., André, I., Dunham, C.M., and Moran, C.P. (2012) Structure of the basal components of a bacterial transporter. *Proc. Nat. Acad. Sci. U. S. A.*, **109**, 5446–5451.
- Pradhan, B., Liedtke, J., Sleutel, M., Lindbäck, T., Zegeye, E.D., K, O.S., Llarena, A.K., Brynildsrud, O., Aspholm, M., and Remaut, H. (2021) Endospore Appendages: a novel pilus superfamily from the endospores of pathogenic Bacilli. *EMBO J.*, e106887.
- Ramírez-Guadiana, F.H., Meeske, A.J., Rodrigues, C.D.A., Barajas-Ornelas, R.D.C., Kruse, A.C., and Rudner, D.Z. (2017) A two-step transport pathway allows the mother cell to nurture the developing spore in *Bacillus subtilis*. *PLoS Genet.*, **13**, e1007015.
- Reynolds, E.S. (1963) The use of lead citrate at high pH as an electron-opaque stain in electron microscopy. *J. Cell Biol.*, **17**, 208–212.
- Rudner, D.Z., and Losick, R. (2001) Morphological coupling in development: lessons from prokaryotes. *Dev. Cell*, **1**, 733–742.
- Sato, T., Samori, Y., and Kobayashi, Y. (1990) The *cisA* cistron of *Bacillus subtilis* sporulation gene *spoIVC* encodes a protein homologous to a site-specific recombinase. *J. Bacteriol.*, **172**, 1092–1098.
- Schindelin, J., Arganda-Carreras, I., Frise, E., Kaynig, V., Longair, M., Pietzsch, T., Preibisch, S., Rueden, C., Saalfeld, S., Schmid, B., Tinevez, J.Y., White, D.J., Hartenstein, V., Eliceiri, K., Tomancak, P., and Cardona, A. (2012) Fiji: an open-source platform for biological-image analysis. *Nat. Methods*, **9**, 676–682.
- Serrano, M., Kint, N., Pereira, F.C., Saujet, L., Boudry, P., Dupuy, B., Henriques, A.O., and Martin-Verstraete, I. (2016) A recombination directionality factor controls the cell type-specific activation of σ^K and the fidelity of spore development in *Clostridium difficile*. *PLoS Genet.*, **12**, e1006312.
- Setlow, B., Atluri, S., Kitchel, R., Koziol-Dube, K., and Setlow, P. (2006) Role of dipicolinic acid in resistance and stability of spores of *Bacillus subtilis* with or without DNA-protective alpha/beta-type small acid-soluble proteins. *J. Bacteriol.*, **188**, 3740–3747.
- Shuster, B., Khemmani, M., Abe, K., Huang, X., Nakaya, Y., Maryn, N., Buttar, S., Gonzalez, A.N., Driks, A., Sato, T., and Eichenberger, P. (2019a) Contributions of crust proteins to spore surface properties in *Bacillus subtilis*. *Mol. Microbiol.*, **111**, 825–843.
- Shuster, B., Khemmani, M., Nakaya, Y., Holland, G., Iwamoto, K., Abe, K., Imamura, D., Maryn, N., Driks, A., Sato, T., and Eichenberger, P. (2019b) Expansion of the spore surface polysaccharide layer in *Bacillus subtilis* by deletion of genes encoding glycosyltransferases and glucose modification enzymes. *J. Bacteriol.*, **201**, e00321-00319.
- Stewart, G.C. (2015) The Exosporium Layer of Bacterial Spores: a Connection to the Environment and the Infected Host. *Microbiol. Mol. Biol. Rev.*, **79**: 437–457.
- Stragier, P., Kunkel, B., Kroos, L., and Losick, R. (1989) Chromosomal rearrangement generating a composite gene for a developmental transcription factor. *Science*, **243**, 507–512.
- Tovar-Rojo, F., Chander, M., Setlow, B., and Setlow, P. (2002) The products of the *spoVA* operon are involved in dipicolinic acid uptake into developing spores of *Bacillus subtilis*. *J. Bacteriol.*, **184**, 584–587.
- Zhang, F., Li, X.L., Zhu, S.J., Ojaghian, M.R., and Zhang, J.Z. (2018) Data on the ultrastructural characteristics of *Paenibacillus polymyxa* isolates and biocontrol efficacy of *P. polymyxa* ShX301.